The American Journal of Pathology, Vol. 182, No. 6, June 2013

ELSEVIER

The American Journal of
PATHOLOGY
ajp.amjpathol.org

NEUROBIOLOGY

A Phenotypic Change But Not Proliferation Underlies Glial Responses in Alzheimer Disease

Alberto Serrano-Pozo,*† Teresa Gómez-Isla,*† John H. Growdon,*† Matthew P. Frosch,*‡ and Bradley T. Hyman*†

From the Massachusetts Alzheimer's Disease Research Center, the C.S. Kubik Laboratory,‡ Department of Pathology, and the Department of Neurology,† Massachusetts General Hospital and Harvard Medical School, Boston, Massachusetts*

Accepted for publication February 21, 2013.

Address correspondence to Bradley T. Hyman, M.D., Ph.D. Alzheimer Research Unit, MassGeneral Institute for Neurodegenerative Diseases, 16th St., Bldg. 114, Charlestown, MA 02129. E-mail: bhyman@partners.org.

Classical immunohistochemical studies in the Alzheimer disease (AD) brain reveal prominent glial reactions, but whether this pathological feature is due primarily to cell proliferation or to a phenotypic change of existing resting cells remains controversial. We performed double-fluorescence immunohistochemical studies of astrocytes and microglia, followed by unbiased stereology-based quantitation in temporal cortex of 40 AD patients and 32 age-matched nondemented subjects. Glial fibrillary acidic protein (GFAP) and major histocompatibility complex II (MHC2) were used as markers of astrocytic and microglial activation, respectively. Aldehyde dehydrogenase 1 L1 and glutamine synthetase were used as constitutive astrocytic markers, and ionized calcium-binding adaptor molecule 1 (IBA1) as a constitutive microglial marker. As expected, AD patients had higher numbers of $GFAP^+$ astrocytes and $MHC2^+$ microglia than the nondemented subjects. However, both groups had similar numbers of total astrocytes and microglia and, in the AD group, these total numbers remained essentially constant over the clinical course of the disease. The GFAP immunoreactivity of astrocytes, but not the MHC2 immunoreactivity of microglia, increased in parallel with the duration of the clinical illness in the AD group. Cortical atrophy contributed to the perception of increased glia density. We conclude that a phenotypic change of existing glial cells, rather than a marked proliferation of glial precursors, accounts for the majority of the glial responses observed in the AD brain. *(Am J Pathol 2013, 182: 2332–2344; http://dx.doi.org/10.1016/j.ajpath.2013.02.031)*

The role of glial cells in Alzheimer disease (AD), particularly the role of astrocytes and microglia, is a matter of growing interest. Pioneering immunohistochemical studies revealed an increased immunoreactivity for astrocytes and microglial cells in the cortex of AD patients, compared with that of nondemented elderly people, with the vast majority of these cells clustering around dense-core plaques.[1,2] Astrocytes are usually visualized with immunohistochemistry for glial fibrillary acidic protein (GFAP), but recent data suggest that only a subset of all astrocytes, labeled with aldehyde dehydrogenase 1 L1 (ALDH1L1), are also GFAP immunopositive.[3,4] Similarly, a number of microglial markers are available that do not completely overlap with one another and that also label blood and bone marrow mononuclear phagocytes,[5] including major histocompatibility complex II [MHC2 (alias HLA-DP-DQ-DR)],[6] CD11b (alias Mac-1, CR3),[7] CD45 [alias leukocyte common antigen (LCA)],[8] ionized calcium-binding adaptor molecule 1 [IBA1; alias allograft inflammatory factor 1 (AIF-1)],[9] and CD68.[10]

In AD, in various other neurodegenerative disorders, and in acute brain injuries such as stroke, trauma or infection, the terms *reactive astrocytes* and *activated microglia* are widely used to describe the characteristic morphology (ie, hypertrophy of soma and retraction and thickening of processes) of these glial cells. However, the astrocytic and microglial reactions observed in these conditions have also been often referred to as *glial proliferation* or *glial hyperplasia*.[11,12] To understand the role of glial cells in AD and their relationship to amyloid plaques and neurofibrillary tangles (NFTs), the pathological hallmarks of AD, it is important to know whether glial responses involve proliferation of glia or are due mainly to a phenotypic change in existing glia. With the present study, we sought to understand the relative contribution of cell proliferation versus phenotypic change to the increased

Supported by NIH grants AG08487 and P50-AG05134 (to B.T.H.). A.S.-P. was awarded a fellowship from Fundación Alfonso Martín Escudero (Madrid, Spain).

http://dx.doi.org/10.1016/j.ajpath.2013.02.031

number of astrocytes and microglial cells described in the AD brain by classical immunohistochemistry.

To this end, we performed double-fluorescence immunohistochemical studies and unbiased stereology-based analyses on the temporal cortex of a large sample of AD patients and age-matched nondemented individuals. Double-labeling of astrocytes with GFAP and glutamine synthetase (GS) or ALDH1L1 enabled the visualization of many astrocytes that were not identifiable with GFAP immunohistochemistry alone, particularly in nondemented subjects. Stereology-based counts revealed that the total number of astrocytes does not differ between AD brain and normal aging brain, and that the number of astrocytes remains essentially constant through the clinical course of AD (although astrocytes increasingly become $GFAP^+$ as the disease progresses). Double-labeling of microglia with IBA1 and MHC2 revealed that there are distinct subpopulations of microglial cells in the cortex, and that the number of $MHC2^+$ activated microglia, but not the total number of microglial cells, is significantly increased in the AD brain. Thus, we conclude that glial responses in AD are largely due to a phenotypic change of resting glial cells, rather than to cell proliferation.

Materials and Methods

Subjects

Clinicodemographic characteristics of the study subjects are summarized in Table 1. Brain specimens of 40 AD patients and 32 nondemented individuals were obtained from the Massachusetts Alzheimer's Disease Research Center brain bank. The 40 AD patients met clinical criteria for probable AD[13] and neuropathological criteria for high likelihood of AD,[14] and were selected on the basis of disease duration from symptom onset ($\leq$5 years, $n = 10$; 6 to 10 years, $n = 10$; 11−15 years, $n = 10$; >15 years, $n = 10$). The 32 nondemented control subjects had no clinical history of neurological disorders and did not meet the pathological criteria for any neurodegenerative disease.

Morphological Studies

Immunohistochemistry

Formalin-fixed, paraffin-embedded sections (8 μm thick) from the temporal polar association cortex (Brodmann area 38) were cleared in xylenes, rehydrated with decreasing concentrations of ethanol, and subjected to a standard antigen-retrieval procedure consisting of a 20 minutes microwaving in boiling citrate buffer (0.01 mol/L, pH 6.0) with 0.05% Tween 20. The sections were cooled at 4°C for approximately 30 to 45 minutes, blocked with 5% normal goat serum at room temperature for 1 hour, and incubated with the primary antibody overnight at 4°C. The next day, the sections were washed three times (for 10 minutes each wash) with Tris-buffered saline and incubated with the appropriate secondary antibodies for 1 hour at room temperature. Finally, the sections were again washed three times (for 10 minutes each wash) with Tris-buffered saline, incubated with DAPI (catalog no. MP01306; Life Technologies−Invitrogen, Carlsbad, CA) for 20 minutes to display the cell nuclei, counterstained with Thioflavin-S 0.05% in ethanol 50% for 8 minutes, differentiated in ethanol 80% for 30 seconds, and then coverslipped with Immu-Mount nonfluorescing aqueous mounting medium (catalog no. 99-904-12; Thermo Scientific, Pittsburgh, PA) or ProLong Gold antifade reagent (catalog no. P36934; Life Technologies−Invitrogen).

Table 1 Clinicodemographic Characteristics of Study Subjects

Characteristic	Nondemented	AD	*P* value
Sample size	$n = 32$	$n = 40$	
Age at death [years (means ± SD)]	81.3 ± 12.6	77.6 ± 8.6	>0.05*
Females [no. (%)]	19 (59.4)	26 (65.0)	>0.05†
Postmortem interval [hours (means ± SD)]	17.9 ± 11.7	14.1 ± 6.2	>0.05‡
APOE ε4 allele carriers [*n*/*N* (%)]	5/27§ (18.5)	21/40 (52.5)	0.0058†

*Unpaired Student's *t*-test with Welch's correction.
†Chi-square with Fisher's exact test.
‡*U*-test.
§*APOE* genotype was not available for five nondemented subjects.

To label astrocytes, rabbit polyclonal anti-GFAP (1:1000; catalog no. G9269; Sigma-Aldrich, St. Louis, MO) was combined with either mouse monoclonal anti-ALDH1L1 (1:50 supernatant; catalog no. 73-164; NeuroMab, UC Davis, Davis, CA) or mouse monoclonal anti-GS (1:1000; clone GS-6, catalog no. MAB302; EMD Millipore, Billerica, MA). Fluorescently labeled secondary antibodies used were Cy3−conjugated goat anti-rabbit and Alexa Fluor 488−conjugated goat anti-mouse (both 1:200; Jackson ImmunoResearch Laboratories, West Grove, PA).

For study of microglia, rabbit polyclonal anti-IBA1 antibody (1:250; catalog no. 019-19741; Wako Pure Chemical Industries, Osaka, Japan) was combined with mouse monoclonal anti−HLA-DP-DQ-DR antibody (1:100; clone CR3/43, catalog no. M0775; Dako, Carpinteria, CA). Secondary antibodies were Alexa Fluor 488−conjugated goat anti-rabbit and Cy3-conjugated goat anti-mouse (both 1:200; Jackson ImmunoResearch Laboratories). To minimize autofluorescence and facilitate the quantitative analysis of microglial cells, the sections doubly stained for IBA1 and MHC2 were treated with an autofluorescence eliminator reagent (catalog no. 2160; EMD Millipore) according to the manufacturer's instructions. Sections not incubated with the primary antibodies served as a negative control in both immunohistochemical studies.

The mitotic marker Ki-67 was used to investigate cell proliferation. Ki-67 is a nuclear protein that is not expressed during the G0 phase but is up-regulated throughout the cell cycle and, thus, unlike cyclins, can label cells in all G1, S, and G2 phases.[15] The Ki-67 antibody (1:50; rabbit monoclonal, clone SP6; catalog no. ab16667; Abcam, Cambridge,

MA) was used in temporal cortex and hippocampal sections pretreated with the antigen-retrieval protocol described above. This antigen-retrieval method has been reported to be very effective for improving the Ki-67-immunoreactive signal in formalin-fixed, paraffin-embedded archival tissue, even when the paraffin blocks have been stored for up to 60 years.[16] After immunohistochemistry, the sections were treated with the same autofluorescence eliminator reagent (EMD Millipore). Sections from an autopsied patient with a high-grade glioma were used as a positive control.

Stereology-Based Quantitative Analyses

Stereology-based studies were performed in single sections per case. Sections were placed on the motorized stage of an Olympus BX51 epifluorescence microscope equipped with a DP70 digital CCD camera, an X-Cite fluorescent lamp, and the associated CAST stereology software version 2.3.1.5 (Olympus, Tokyo, Japan). The cortical ribbon of the specimen was outlined with the appropriate tool of this software under the 4× objective, and this region of interest was randomly sampled using the optical disector probe of the software. For astrocytes, the stereology-based counts were performed under the 20× objective, with a meander sampling of 1% and a counting frame of 14,260 μm^2 area (10%). For microglia, we used a 40× objective, a meander sampling of 1% to 4%, and a counting frame of 3565 μm^2 area (10%). The random sampling protocol was designed to cover the entire cortical ribbon of the specimen with an even representation of the six cortical layers and with an endpoint of at least 100 cells. A dual-band filter cube fluorescein isothiocyanate/Cy3 (U-N51009; Chroma Technology, Brattleboro, VT) designed for the simultaneous visualization of these two fluorophores was used to examine immunoreactivity for the pairs of astrocytic or microglial markers mentioned above.

Only glial cells with the cell soma and DAPI-positive visible nucleus inside the counting frame or outside but touching either of the two green sides were counted; those with the cell soma touching either of the red sides of the counting frame were excluded from the count. During quantification of microglia, cells immunoreactive for IBA1 or MHC2 that were located within vessels or in their immediate vicinity were interpreted as blood mononuclear phagocytes and perivascular macrophages, respectively, and were not counted. The distance between each microglial cell and the closest Thioflavin-S−positive dense-core plaque or NFT was obtained with the appropriate tool of the CAST software, and microglial cells were then classified as close, if located within 50 μm, or as far, if located beyond this boundary.

Counts were performed under masking to clinical data (diagnosis, disease duration, *APOE* genotype). The density of astrocytes and of microglial cells was calculated as the number of cells of each type counted, divided by the total area sampled (number of disectors × counting frame size). To prevent the enhancing effect of disease-related cortical atrophy on density values in the AD group, these values were then corrected by the average cortical thickness of the specimen and normalized to a 1 cm-long strip of full-width cortex to obtain a total number of astrocytes and microglial cells.

The cortical thickness was obtained as described previously.[17] Briefly, sections were placed under the 1.6× objective of the microscope and the full thickness of the cortical ribbon was measured with the appropriate tool of the CAST software in 20 random sites throughout the specimen. Cortical thickness was estimated as the average of these 20 measurements.

Statistical Analysis

Normality of data sets was evaluated with the D'Agostino−Pearson omnibus test. Pairwise comparisons were performed with a *U*-test when either of the two data sets was not normally distributed, and with an unpaired Student's *t*-test when both were normally distributed. In the latter, Welch's correction was applied when the variances were significantly different according to the *F*-test. Correlations between number of astrocytes or microglial cells and disease duration, age of death, and postmortem interval were performed with Pearson's correlation test or with Spearman's sum rank correlation, when appropriate. Comparisons between microglia counts close to and far from plaques and NFTs were performed with a one-tailed Wilcoxon signed rank test or a one-tailed paired *t*-test, when appropriate. All other tests were two-sided. The significance level was set at $P < 0.05$. All statistical analyses were performed using GraphPad Prism for Mac software version 5.0 (GraphPad Software, La Jolla, CA).

Results

Phenotypic Change But Constant Number of Astrocytes in AD

To investigate whether the enhanced GFAP immunoreactivity observed in AD is due to astrocyte proliferation or whether it indicates a phenotypic change from resting $GFAP^-$ astrocytes to reactive $GFAP^+$ astrocytes, we performed double-fluorescence immunostaining for GFAP and ALDH1L1 in the temporal association cortex of 40 AD patients and 32 nondemented control subjects. ALDH1L1 is a glycolytic enzyme isoform expressed mainly in astrocytes.[3,4] Preliminary inspection revealed that ALDH1L1 positivity is useful for detecting many astrocytes that would be otherwise undetectable with GFAP immunostaining alone, particularly in nondemented control subjects; in the AD group, as expected, most astrocytes were also $GFAP^+$ (Figure 1). Thus, we distinguished two main populations of astrocytes: $ALDH1L1^+GFAP^-$ (resting astrocytes) and $ALDH1L1^+GFAP^+$ (reactive astrocytes).

Using unbiased stereology-based quantitation, we observed that the total number of astrocytes did not differ significantly between the nondemented and the AD groups ($P = 0.3616$) (Figure 2A). As expected, the number of

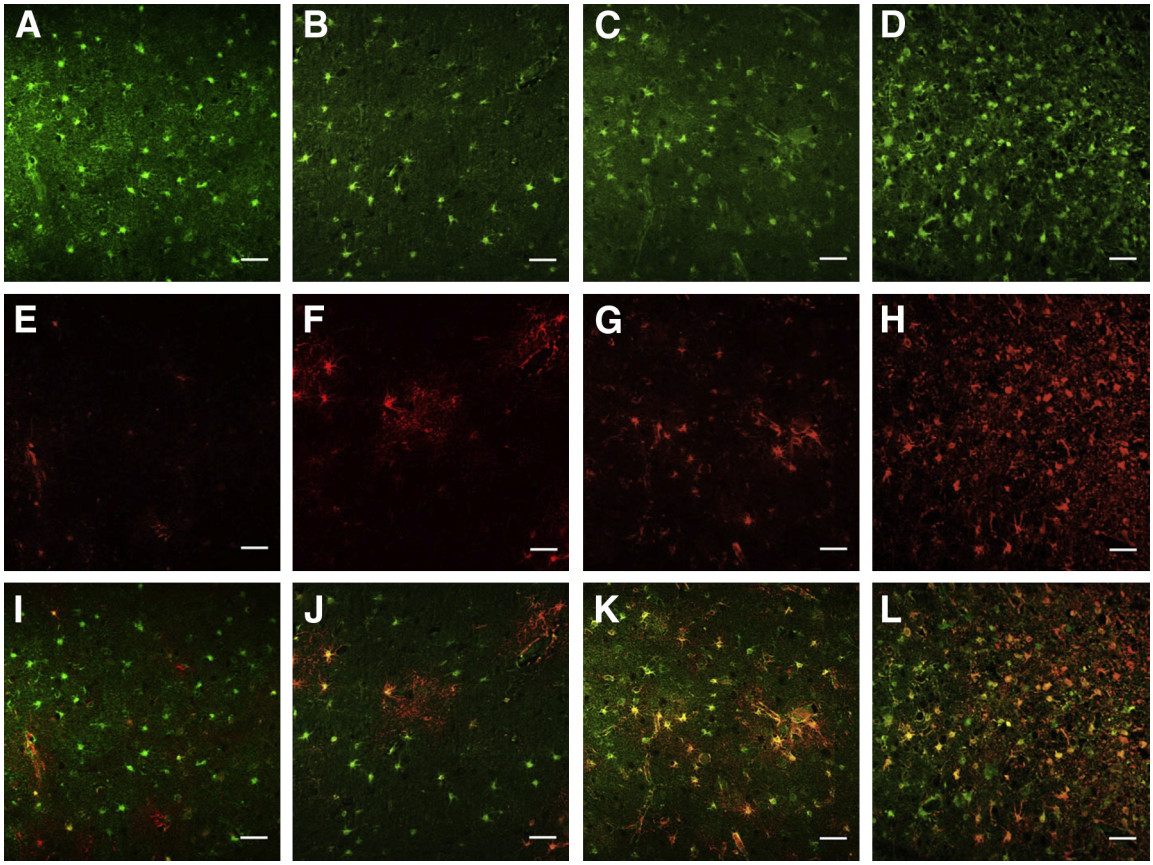

Figure 1 Confocal images representative of double-fluorescence immunohistochemical study of astrocytes with ALDH1L1 (green) (**A**–**D**) and GFAP (red) (**E**–**H**); merged images are also shown (**I**–**L**). Representative images from four cases are shown: one nondemented control subject (**A**, **E**, and **I**), and three AD patients with 5 years (**B**, **F**, and **J**), 12 years (**C**, **G**, and **K**), and 19 years (**D**, **H**, and **L**) of clinical illness. The majority of astrocytes in the nondemented individual were $GFAP^-$ (resting astrocytes), as seen in the merged image (**I**), whereas astrocytes in the AD cortex displayed a reactive phenotype with GFAP-immunoreactivity that was associated with the duration of the illness (**J**, **K**, and **L**). Disease-related cortical atrophy produced an increase in the density of astrocytes (green) (**A** versus **D**). Scale bar = 50 μm.

reactive $GFAP^+$ astrocytes was much higher in the AD group ($P = 0.0082$) (Figure 2E). By contrast, the number of resting $ALDH1L1^+GFAP^-$ astrocytes was substantially lower ($P = 0.0033$) (Figure 2C). To evaluate whether these changes track with disease severity, we performed correlations between cell counts and disease duration from symptom onset within the AD group. We have previously used disease duration from symptom onset as a reliable proxy of dementia severity in AD. Disease duration has the advantage of avoiding the floor effect of neuropsychological testing in patients with severe dementia, who are typically not testable. Furthermore, in our previous neuropathological studies we have observed that disease duration correlates with the burden of NFTs[18] and with the extent of neuron loss,[19] synaptic loss,[20] and cortical atrophy,[21] which are the strongest pathological correlates of cognitive decline in AD. Moreover, unlike categorical variables such as Braak stage of NFTs, duration of illness is inherently a continuous linear variable. The correlations with duration of clinical illness revealed that the number of $ALDH1L1^+GFAP^+$ reactive astrocytes increased linearly ($r = 0.4768$, $P = 0.0019$) (Figure 2F), just as the number of $ALDH1L1^+GFAP^-$ resting astrocytes decreased ($r = -0.4884$, $P = 0.0014$) (Figure 2D), but the total number of astrocytes remained essentially unchanged after symptom onset, despite disease progression ($r = 0.2276$, $P = 0.1579$) (Figure 2B).

We sought to confirm these results with another astrocytic marker, GS. This enzyme catalyzes the conversion of glutamate into glutamine in the astrocytic cytoplasm. Inspection of the double-stained sections revealed a pattern similar to that with ALDH1L1/GFAP double immunostaining (Figure 3), and the results of the stereology-based quantitative analyses reached a higher significance level than those of the ALDH1L1/GFAP quantification (Figure 4). The total number of astrocytes did not differ significantly between nondemented subjects and AD patients ($P = 0.8932$), and did not increase over the course of AD ($r = 0.1109$, $P = 0.4958$); by contrast, the number of GS^+GFAP^- astrocytes was significantly higher in the nondemented group ($P < 0.0001$) and the number of GS^+GFAP^+ astrocytes was significantly higher in the AD group ($P < 0.0001$). Moreover, the number of GS^+GFAP^- astrocytes decreased as the number of GS^+GFAP^+ astrocytes increased over the course of AD ($r = -0.4870$, $P = 0.0014$, and $r = 0.4179$, $P = 0.0073$, respectively). In fact, we observed a strong correlation

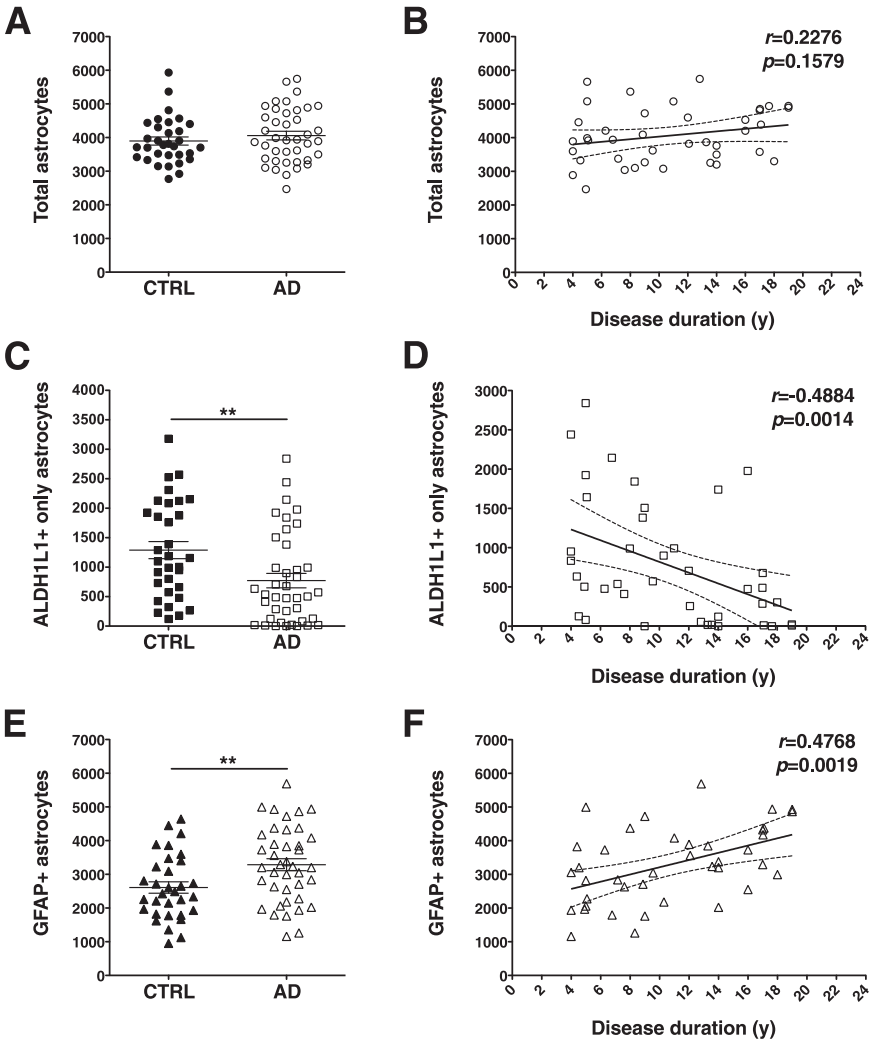

Figure 2 Stereology-based quantitative analysis of astrocytes double-labeled for ALDH1L1 and GFAP. The total number of astrocytes did not differ between AD patients and nondemented control (CTRL) subjects (**A**) and remained essentially constant through the disease clinical course (**B**). The number of ALDH1L1^{+}GFAP^{+} astrocytes was higher in the AD group (**E**), whereas the number of ALDH1L1^{+}GFAP^{-} astrocytes was higher in the nondemented group (**C**). Astrocytes became increasingly reactive (GFAP^{+}) as the clinical phase of the disease advances (**D** and **F**). Counts in each case are not density measures, but estimates of the number of cells per 1 cm-long full-width cortex from a single section of temporal isocortex. Data are expressed as individual values with means ± SEM (**A**, **C**, and **E**) or 95% confidence interval of the mean slope (**B**, **D**, and **F**). $^{**}P < 0.01$.

between the measures of total astrocytes obtained with the ALDH1L1/GFAP and the GS/GFAP double immunohistochemistry ($r = 0.6141$, $P < 0.0001$), and also between the number of ALDH1L1^{+}GFAP^{-} astrocytes and the number of GS^{+}GFAP^{-} astrocytes ($r = 0.8629$, $P < 0.0001$).

Although GS is constitutively expressed in astrocytes, it has also been reported to stain pyramidal neurons in the cortex of AD patients.[22] Indeed, we observed GS^{+} pyramidal neurons in 32 of the 40 AD specimens, typically distributed in foci as described previously,[22] but also in 19 of the 32 nondemented subjects. GS^{+} neurons were easy to distinguish from GS^{+} astrocytes by morphological criteria. Using our stereology-based protocol, we quantified the number of GS^{+} neurons in this sample of AD and nondemented subjects, and found a trend toward a higher number of GS^{+} neurons in the AD group compared with the nondemented group (471 ± 110 versus 325 ± 101 GS^{+} neurons, means ± SEM; $P = 0.0821$). Moreover, we observed a statistically significant spatial association of GS^{+} neurons to the vicinity (within 50 μm) of Thioflavin-S−positive dense-core plaques in the AD group (296 ± 75 GS^{+} neurons close to plaques versus 175 ± 43 GS^{+} neurons far from plaques; $P = 0.0170$). Only a few of the GS^{+} neurons in the AD group contained a Thioflavin-S−positive NFT (7 ± 4 GS^{+}ThioS^{+} neurons).

Phenotypic Change But Constant Number of Microglia in AD

Three subtypes of microglial cells could be identified according to their immunoreactivity in a preliminary inspection of the IBA1/MHC2 double immunohistochemistry. IBA1^{+}MHC2^{-} cells were the most abundant subtype in the temporal cortex from nondemented subjects, whereas AD specimens had variable amounts of IBA1^{+}MHC2^{+} cells. Interestingly, some AD cases also exhibited IBA1^{-}MHC2^{+} cells (Figure 5). We can assume that these cells were not confounded with circulating mononuclear blood cells or with perivascular macrophages, because they were located in the midst of the neuropil (ie, not within a vessel or in its immediate proximity) and had a similar morphology to that of activated microglia. Although the nature of this third subtype awaits further characterization (as discussed below), here we present

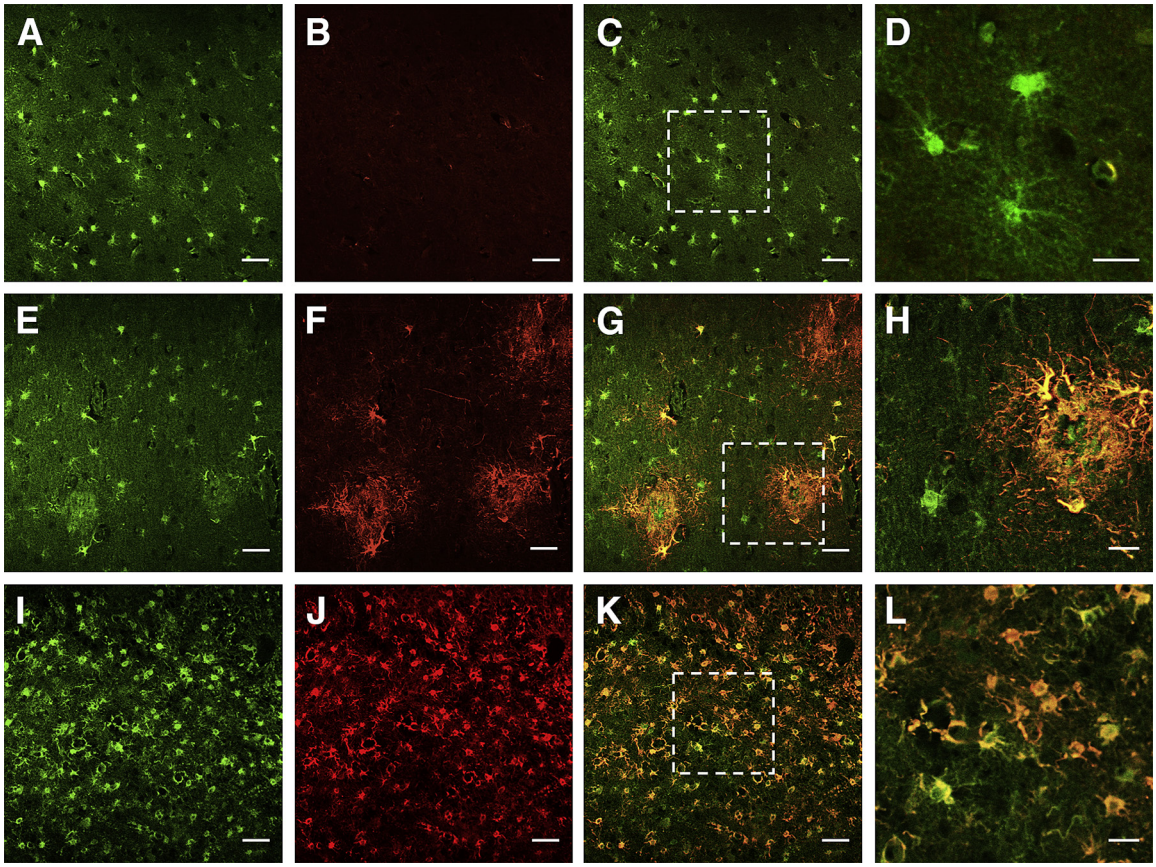

Figure 3 Confocal images of the double-fluorescence immunohistochemical study of astrocytes with GS (green) (**A**, **E**, and **I**) and GFAP (red) (**B**, **F**, and **J**). In merged images (**C**, **G**, and **K**), the **boxed region** is shown at higher magnification in the next panel (**D**, **H**, **L**). Representative images from three cases are shown: one nondemented control subject (**A**–**D**) and two AD patients with 5 years (**E**–**H**) and 19 years (**I**–**L**) of clinical illness. Many astrocytes in nondemented subjects were positive only for GS (**C** and **D**), whereas astrocytes in AD patients exhibited an increased immunoreactivity for GFAP that was associated with the progression of the disease (**G**, **H**, **K**, and **L**). Disease-related cortical atrophy produced an increase in the density of astrocytes (eg, **A** versus **I**). Scale bars: 50 μm (**A**–**C**, **E**–**G**, and **I**–**K**); 20 μm (**D**, **H**, and **L**).

the quantitative results of these three subpopulations of microglia, as well as those of total microglia.

We have previously shown in a larger sample of AD cases that the number of $CD68^+$ microglial cells is increased in AD, compared with normal aging, and that this increase parallels the clinical course of the AD dementia and is not influenced by *APOE* genotype or by cause of death.[21] In the present study, however, using the microglial markers IBA1 and MHC2, we found that the total number of microglia did not differ significantly between the AD and the control groups ($P = 0.8428$) (Figure 6A), which parallels our present findings for astrocytes. Moreover, the number of total microglial cells remained essentially unchanged through the clinical course of the disease ($r = -0.2615$, $P = 0.1031$) (Figure 6B). By contrast, the number of $IBA1^+MHC2^-$ microglia was significantly decreased ($P = 0.0239$; Figure 6C), whereas the number $IBA1^-MHC2^+$ microglia was highly significantly increased ($P < 0.0001$) in the AD group (Figure 6G), compared with the nondemented group. A statistically nonsignificant increase in the number of $IBA1^+MHC2^+$ microglia was also observed in the AD group ($P = 0.1417$) (Figure 6E). However, unlike astrocytes, for microglia the amount of these phenotypic subsets was not predicted by the duration of clinical illness (Figure 6, D, F, and H).

We next studied the spatial distribution of microglial cells with respect to dense-core, Thioflavin-S positive plaques and Thioflavin-S positive NFTs. Based on our previous work,[21] we selected a 50-μm boundary from the closest plaque or NFT to classify microglial cells as close or far. The three subsets of microglial cells were similarly associated with the core pathological lesions of AD, suggesting a similar chemoattractive behavior ($P \leq 0.0001$) (Figure 7).

Several factors have been reported to influence cortical MHC2 immunoreactivity. A long postmortem interval (PMI) can decrease the levels of MHC2, and a death from chronic debilitating diseases such as disseminated cancer or sepsis, can up-regulate MHC2 in the cortex in the absence of AD pathology.[23] However, we observed no correlation between total $MHC2^+$ cell counts and PMI either in the AD group ($r = 0.0972$, $P = 0.5506$) or the nondemented control group ($r = 0.0223$, $P = 0.9049$), and no significant differences between subjects with sudden death (typically myocardial infarction or pulmonary embolism) and those with protracted death (either cancer or sepsis) (data not shown).

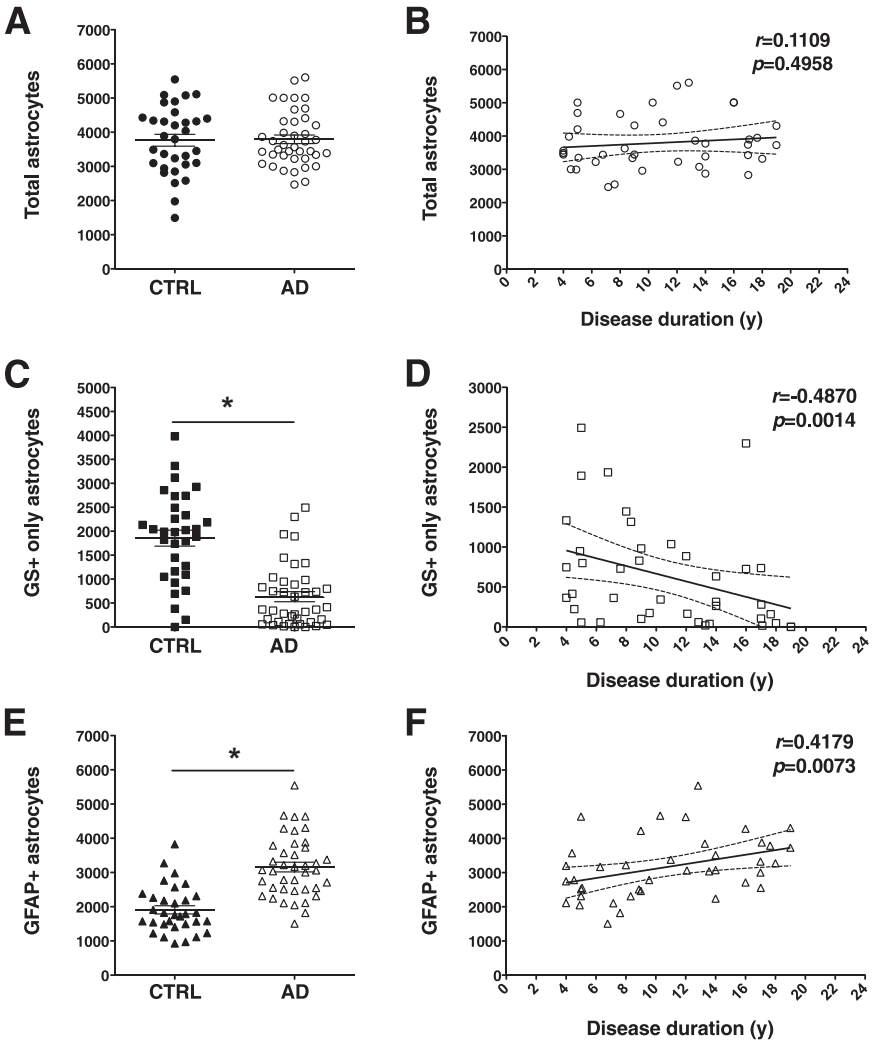

Figure 4 Stereology-based quantitative analysis of astrocytes double-labeled for GS and GFAP. The number of $GS^{+}GFAP^{+}$ astrocytes was higher in the AD group (**E**), whereas the number of $GS^{+}GFAP^{-}$ astrocytes was higher in the nondemented group (**C**), but the number of total astrocytes did not differ significantly between AD patients and nondemented subjects (**A**). This phenotypic change paralleled the progression of the disease, but the number of total astrocytes remained essentially constant through its clinical course (**B**, **D**, and **F**). Counts in each case are not density measures, but estimates of the number of cells per 1 cm-long full-width cortex from a single section of temporal isocortex. Data are expressed as individual values with means ± SEM (**A**, **C**, and **E**) or 95% confidence interval of the mean slope (**B**, **D**, and **F**). $^{*}P < 0.0001$.

Similarly, we observed no effect of sex or age at death (data not shown).

A previous study revealed an *APOE* ε4 allele dose-dependent increase in MHC2 immunoreactivity in *APOE* ε4 carriers, even after adjusting for the extent of AD pathology.[24] We also observed a significantly higher total number of $IBA1^{+}MHC2^{+}$ microglial cells ($P = 0.0061$) and a trend toward significantly fewer $IBA1^{+}MHC2^{-}$ microglial cells ($P = 0.0936$) in AD patients carrying the *APOE* ε4 allele, compared with noncarriers, but there was no difference between genotypes for the subset of $IBA1^{-}MHC2^{+}$ microglia ($P = 0.6524$) or for total number of microglial cells ($P = 0.5333$) (Figure 8).

Increased Density of Total Astrocytes and Microglial Cells Is Due to Cortical Atrophy

Although our results are in agreement with numerous classical immunohistochemical studies reporting increased GFAP and MHC2 immunoreactivity in AD, they argue against the long-established idea that there is an actual increase in the total numbers of astrocytes and microglial cells in AD. A principle of stereology is that the total number of objects provides different information than the density of objects, because brain atrophy by itself can lead to an artificial increase in the density of the object.[25] We therefore asked whether AD-related cortical atrophy possibly distorts the perception of increased GFAP and MHC2 immunoreactivity, thereby contributing to the idea of glial cell proliferation in the AD brain. In the AD group, the expected cortical atrophy was present in the temporal cortex of our AD group (Figure 9A), and cortical atrophy was strongly correlated with duration of clinical illness (Figure 9D). To evaluate the effect of cortical atrophy, we compared the density measures of astrocytes and microglial cells from the AD and nondemented groups, instead of comparing only the cell counts corrected by cortical thickness as above. These analyses revealed that the densities of all astrocytes and microglial cells were significantly higher in AD patients, compared with nondemented subjects. These statistically significant results were due mainly to expected larger differences in the densities of $GFAP^{+}$ astrocytes and $MHC2^{+}$ microglia, but also to smaller differences in the densities of $GFAP^{-}$ astrocytes and $MHC2^{-}$ microglia (data not shown). Within the

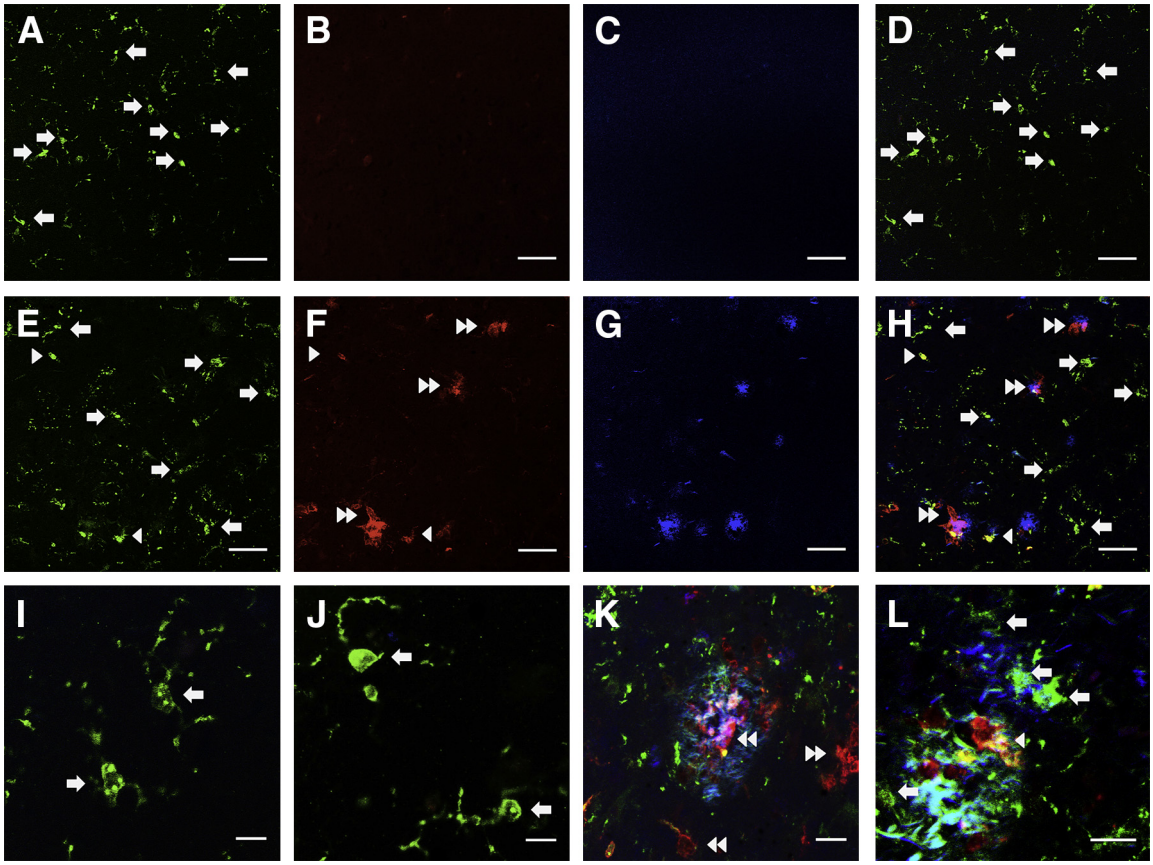

Figure 5 Confocal images of the double-fluorescence immunohistochemical study of microglia with IBA1 (green) (**A** and **E**) and MHC2 (red) (**B** and **F**). Representative images from a nondemented subject (**A**–**D**) and an AD patient (**E**–**H**) are shown. Also shown are merged high-power images from two different nondemented individuals (**I** and **J**) and from two different AD patients (**K** and **L**). Thioflavin-S staining (blue-green) identifies plaques (**G**, **H**, **K**, and **L**). The uniform morphology and labeling of microglia in nondemented subjects contrasts with the morphological and molecular diversity of microglia in AD. Three subpopulations of microglial cells are discernible with this double labeling: $IBA1^{+}MHC2^{-}$ (**arrows**), $IBA1^{+}MHC2^{+}$ (**arrowheads**), and $IBA1^{-}MHC2^{+}$ (**double arrowheads**) cells. Scale bars: 50 μm (**A**–**H**); 20 μm (**K** and **L**); 10 μm (**I** and **J**).

AD group, correlations with duration of clinical illness also yielded a significant increase of the density of all astrocytes over the clinical course of the disease (Figure 9D), due mainly to a stronger positive correlation of $GFAP^{+}$ astrocytes, but also to a slightly weaker negative correlation of $GFAP^{-}$ astrocytes (data not shown). No significant correlation with disease duration was observed for the density of all microglia (Figure 9D) or of any of the microglial subpopulations (data not shown).

Discussion

Phenotypic Change versus Proliferation of Glial Cells in AD

Astrocytes and microglial cells are thought to actively sense their local environment, reacting to any injury within their domain of influence. Whether this reaction involves generation of new glial cells remains controversial. Recently, for example, a staging of astrocytic reaction based on GFAP immunoreactivity has been proposed in which proliferation is considered a feature characteristic of advanced AD, in the context of diffuse severe reaction and formation of compact glial scars around amyloid plaques.[12] Here, we provide evidence suggesting that the increase in reactive glia in the AD brain is due largely to a phenotypic change of existing resting glial cells, rather than to generation of new glial cells from glial precursors. Two technical features particular to the present study enabled us to reach this conclusion: one is the use of double-fluorescence immunohistochemistry combining antibodies against constitutive and activation markers of astrocytes and microglia, rather than the standard single-antibody immunohistochemistry for the classical markers of reactive glia, GFAP and MHC2; the other is the use of stereology-based quantitative methods, including systematic and random sampling of the specimens to avoid observer bias, and estimation of cell counts corrected by cortical atrophy rather than density measures, which can be artificially enhanced in the context of a reduced volume of cortex.[25]

The evidence for generation of new glial cells in AD is conflicting. A previous stereology-based human postmortem study using Nissl staining for neurons and analyzing the morphology of the stained cells revealed no difference in the

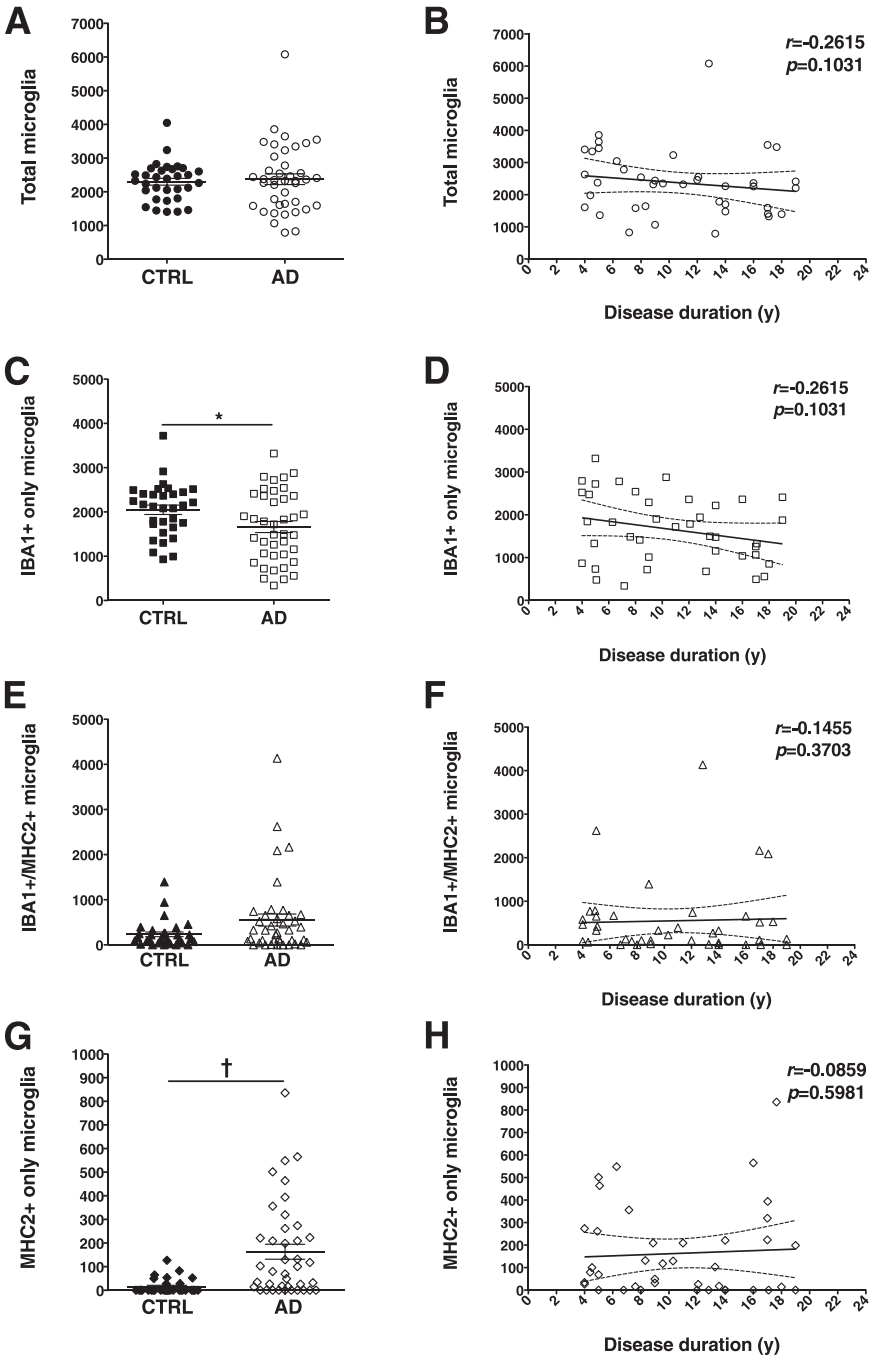

Figure 6 Stereology-based quantitative analysis of microglia double-labeled for IBA1 and MHC2. The total number of microglia did not differ significantly between the nondemented and the AD groups (**A**). Within the AD group, neither total microglial cells (**B**) nor any of the microglia subtypes (**D**, **F**, and **H**) was observed to increase with the clinical progression of the disease. However, $IBA1^{+}MHC2^{-}$ microglia (**C**) was significantly more abundant in the nondemented group, and $IBA1^{-}MHC2^{+}$ microglia (**G**) were significantly more abundant in the AD. There was a trend toward increase in $IBA1^{+}MHC2^{+}$ microglia in the AD group (**E**). Counts in each case are not density measures, but estimates of the number of cells per 1 cm-long full-width cortex from a single section of temporal isocortex. Data are expressed as individual values with means ± SEM (**A**, **C**, **E**, and **G**) or 95% confidence interval of the mean slope (**B**, **D**, **F**, and **H**).*$P < 0.05$, †$P < 0.0001$.

number of astrocytes and microglial cells in AD, compared with age-matched nondemented individuals.[26] Reports of other studies, however, have described an increased expression of cell division markers, including Ki-67 and cyclins, by astrocytes in the AD brain[27–29] and in an APP-overexpressing mouse model.[30] More dynamic animal studies with injections of bromodeoxyuridine have shown that the number of bromodeoxyuridine-positive glial cells is increased in APP transgenic mice, compared with their wild-type littermates, particularly in the vicinity of plaques, and the majority of these bromodeoxyuridine-positive cells were identified as microglia, rather than astrocytes.[31–33]

Given the cross-sectional design inherent to any neuropathological study, the finding of similar total numbers of astrocytes and microglial cells in AD patients and nondemented subjects could also be explained by a balance between cell proliferation and death. However, this possibility seems less likely, because we noticed a wide range of intermediate phenotypes in individual glial cells with our double-fluorescent stainings, ranging from no GFAP or MHC2 immunoreactivity to very intense immunoreactivity (Figures 1, 3, and 5), favoring the idea of phenotypic change, and also because we failed to observe a significant positive fluorescent staining with the mitotic marker Ki-67

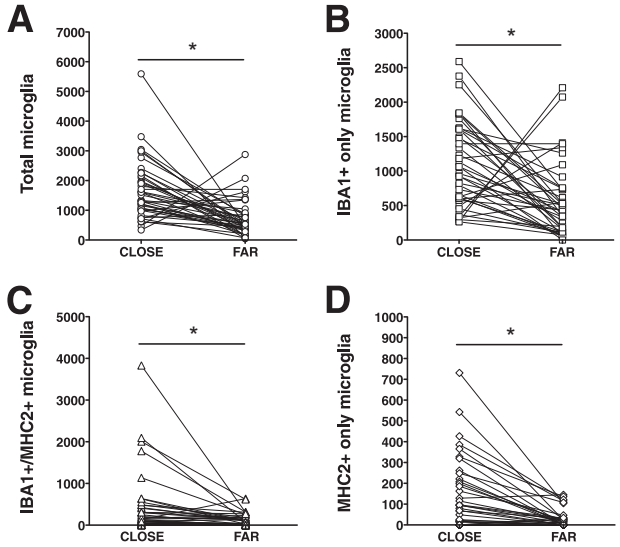

Figure 7 Association of the three microglial subpopulations with dense-core plaques and NFTs. The randomly selected microglial cells were categorized as close if located within 50 μm from the closest dense-core plaque or NFT, or as far if located more than 50 μm away from it. The three subsets of microglial cells are similarly attracted by the pathological hallmarks of AD and recruited toward them. Counts in each case are not density measures, but estimates of the number of cells per 1 cm-long full-width cortex from a single section of temporal isocortex. Counts close and far (from AD pathological hallmarks) from each of the 40 AD subjects are connected with lines. $^{*}P < 0.0001$.

in both the AD and nondemented subjects, whether in the temporal neocortex or in the hippocampus (Supplemental Figure S1). Although Ki-67 is widely used to assess the proliferative capacity of brain tumors, the number of positive cells in the normal or AD brain at any given moment may be too low and therefore this approach would require an exhaustive and time-consuming sampling of the entire brain.

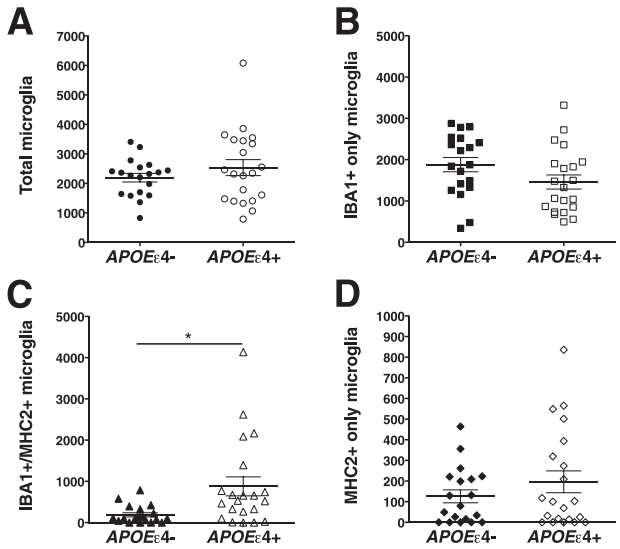

Figure 8 Effect of the *APOE* ε4 allele on microglial phenotype. Numbers of total microglia (**A**), $IBA1^{+}MHC2^{-}$ microglia (**B**), and $IBA1^{-}MHC2^{+}$ microglia (**D**) did not differ between *APOE* ε4 carriers and noncarriers. Only for $IBA1^{+}MHC2^{+}$ microglia (**C**) were numbers significantly higher in *APOE* ε4 carriers, compared with noncarriers. Counts in each case are not density measures, but estimates of the number of cells per 1 cm-long full-width cortex from a single section of temporal isocortex. Data are expressed as individual values with means ± SEM. $^{*}P < 0.01$.

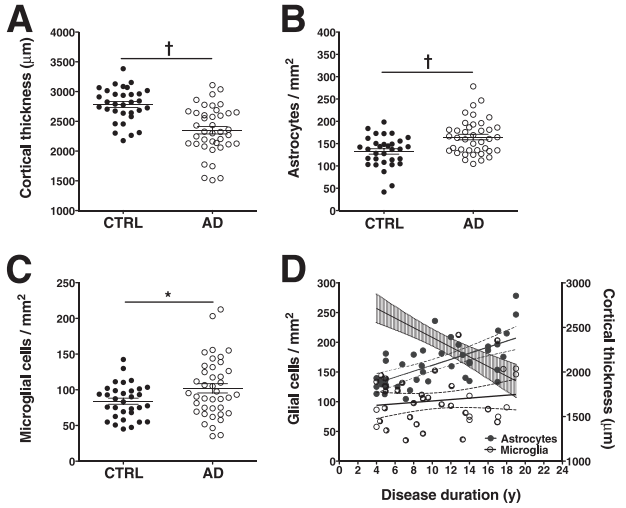

Figure 9 Effect of cortical atrophy on density measures of astrocytes and microglia. **A**: As expected, the quantification of cortical thickness of the temporal isocortex (Brodmann area 38) in the study subjects revealed significant cortical atrophy in the AD group, compared with the nondemented group. **B** and **C**: Unlike total numbers (Figures 2, 4, and 6), densities of total astrocytes (**B**) and total microglial cells (**C**) were significantly increased in the AD group, compared with the nondemented group. **D**: In the AD group, cortical thickness (**right** *y* axis and regression line with **shaded error bars**) correlated negatively with duration of clinical illness ($r = -0.6538$, $P < 0.0001$), indicating that disease duration is a reliable proxy of dementia severity. Unlike the total number of astrocytes (Figures 2 and 4), density (**left** *y* axis) of all astrocytes (solid symbols) correlated positively with disease duration ($r = 0.6400$, $P < 0.0001$), because of progressive cortical atrophy; however, density of all microglia (open symbols) did not correlate significantly with disease duration ($r = 0.0982$, $P = 0.5466$). The 95% confidence interval (open error bars) of the mean slope is indicated. Data used to build the cortical thickness regression line for these 40 AD patients were drawn from Serrano-Pozo et al.[21] $^{*}P < 0.05$, $^{\dagger}P < 0.0001$.

Implications for the Role of Glia in AD

The distinction between phenotypic change and proliferation as contributors to glial reactions is not merely semantic, but has relevant pathophysiological implications. We have recently shown that the number of $GFAP^{+}$ astrocytes and $CD68^{+}$ microglial cells in the temporal neocortex increases linearly through the clinical course of AD and parallels the increasing number of NFTs, whereas amyloid plaque burden remains relatively stable.[21] We also observed that this reactive glia accumulates in the proximity of both dense-core plaques and NFTs.[21] In addition, it has been reported that the number of $GFAP^{+}$ astrocytes correlates with the Braak stage of NFTs,[34] and we and other researchers have shown that cortical GFAP levels measured by enzyme-linked immunosorbent assay correlate with indicators of disease progression, such as duration of clinical disease[20] and cognitive measures.[35] Although this evidence can be interpreted simply as a protective reaction of glial cells to

the ongoing neurodegenerative process, another possible interpretation is that reactive glia in fact contributes to the synaptic and neuronal damage that underlies cognitive impairment in AD.[36] Both astrocytes and microglia have been recently shown to be involved in the normal development of synapses and neuronal circuits during postnatal brain development,[37–39] and they may play an active role in neurodegeneration as well.[40–43] Thus, understanding and manipulating the intimate molecular mechanisms responsible for this phenotypic change should help to elucidate whether glia in AD is protective, is deleterious, or has a dual role.

The identification of a subpopulation of $IBA1^{-}MHC2^{+}$ microglia using double immunofluorescence must be interpreted in the context of what is known about the expression of these markers. IBA1 is thought to be constitutively expressed in resting microglial cells and to become up-regulated on microglial activation.[9] Activated microglia shares expression of MHC2 with blood mononuclear cells, and it is possible that some of the $IBA1^{-}MHC2^{+}$ cells counted were not actually microglial cells but instead were monocytes, lymphocytes, or perivascular macrophages. This explanation seems unlikely, however, because care was taken to exclude positive cells within blood vessels or immediately adjacent to them [ie, perivascular macrophages, known to be MHC-positive[44,45]], because only cells with evident cytoplasmic processes such as those of microglia were included in the counting, and because most of these cells were intimately associated with dense-core plaques (Figures 5 and 7D). It is possible that $IBA1^{-}MHC2^{+}$ cells are indeed peripheral blood cells recruited to the brain parenchyma and modified toward a microglial phenotype. Whether bone marrow–derived circulating mononuclear phagocytes can cross the blood–brain barrier is a matter of intense research and controversy. Studies in plaque-bearing mice models of AD involving whole-body irradiation and transplantation of labeled bone-marrow hematopoietic precursors revealed that these transplanted cells readily enter in the brain and contribute to plaque clearance.[46–48] However, a more recent study comparing whole-body irradiation versus an irradiation protocol with protection of the head has shown that the integrity of the blood–brain barrier may have been compromised by the head irradiation in these prior studies.[49] On the other hand, as suggested by postmortem immunohistochemical studies with antibodies against plasma proteins[50–52] and by an increased cerebrospinal fluid/plasma albumin ratio,[53–55] the integrity of the blood–brain barrier may be impaired in AD patients, compared with age-matched control subjects, and this disruption may be severe enough to facilitate not only the leakage of plasma proteins to the brain parenchyma, but also the recruitment of circulating blood mononuclear phagocytes.

Likewise interesting is the finding that, compared with noncarriers, AD *APOE* ε4 carriers had significantly more $IBA1^{+}MHC2^{+}$ microglia, but similar total numbers of microglial cells. Egensperger et al[24] had already reported this increased MHC2 immunoreactivity in *APOE* ε4 carriers in 1998, and showed that it is independent of the amount of AD pathology. Recent studies have suggested that Apo-E isoforms may differentially influence the innate immune response, with Apo-E4 causing reduced microglial migration[56] and increased proinflammatory activation,[57,58] compared with Apo-E3. Further studies are needed to address the role of Apo-E in microglial expression of MHC2 in AD.

Implications for Imaging Biomarkers of AD

Our findings also have potential implications for development of imaging diagnostic biomarkers. They provide both a rationale and a methodological basis for validation of molecular targets of glia-directed positron emission tomography (PET) radiotracers in postmortem brains. Although it is clear that only radiotracers that target glial receptors specifically up-regulated in cells with the reactive phenotype will be clinically useful as diagnostic and progression biomarkers of AD, the development of glia-directed PET radiotracers has proved to be very challenging. The peripheral benzodiazepine receptor [PBR; alias 18-kDa translocator protein (TSPO)] is considered the preferred molecular target of reactive glia,[59–61] but the first TSPO-directed radiotracer, [^{11}C](*R*)-PK11195, has largely failed to distinguish between AD patients and cognitively intact elderly people.[62,63]

In summary, our results indicate that the higher immunoreactivity observed in AD brain with the classical markers widely used for astrocytes and microglial cells reflects a change in phenotype more than an increase in the absolute number of these cells. Thus, we conclude that both astrocytic and microglial reactions in AD are due largely to a phenotypic change of existing resting glial cells, rather than to a generation of new glial cells from glial precursors.

Acknowledgment

We thank the patients and relatives involved in research at the Massachusetts Alzheimer's Disease Research Center.

Supplemental Data

Supplemental material for this article can be found at *http://dx.doi.org/10.1016/j.ajpath.2013.02.031*.

References

1. Beach TG, Walker R, McGeer EG: Patterns of gliosis in Alzheimer's disease and aging cerebrum. Glia 1989, 2:420–436
2. Itagaki S, McGeer PL, Akiyama H, Zhu S, Selkoe D: Relationship of microglia and astrocytes to amyloid deposits of Alzheimer disease. J Neuroimmunol 1989, 24:173–182
3. Cahoy JD, Emery B, Kaushal A, Foo LC, Zamanian JL, Christopherson KS, Xing Y, Lubischer JL, Krieg PA, Krupenko SA, Thompson WJ, Barres BA: A transcriptome database for astrocytes, neurons, and oligodendrocytes: a new resource for understanding brain development and function. J Neurosci 2008, 28:264–278

4. Zamanian JL, Xu L, Foo LC, Nouri N, Zhou L, Giffard RG, Barres BA: Genomic analysis of reactive astrogliosis. J Neurosci 2012, 32:6391−6410
5. Ulvestad E, Williams K, Mørk S, Antel J, Nyland H: Phenotypic differences between human monocytes/macrophages and microglial cells studied in situ and in vitro. J Neuropathol Exp Neurol 1994, 53: 492−501
6. McGeer PL, Itagaki S, Tago H, McGeer EG: Reactive microglia in patients with senile dementia of the Alzheimer type are positive for the histocompatibility glycoprotein HLA-DR. Neurosci Lett 1987, 79: 195−200
7. Akiyama H, McGeer PL: Brain microglia constitutively express beta-2 integrins. J Neuroimunol 1990, 30:81−93
8. Masliah E, Mallory M, Hansen L, Alford M, Albright T, Terry R, Shapiro P, Sundsmo M, Saitoh T: Immunoreactivity of CD45, a protein phosphotyrosine phosphatase, in Alzheimer's disease. Acta Neuropathol 1991, 83:12−20
9. Ito D, Imai Y, Ohsawa K, Nakajima K, Fukuuchi Y, Kohsaka S: Microglia-specific localization of a novel calcium binding protein, Iba1. Brain Res Mol Brain Res 1998, 57:1−9
10. Verbeek MM, Otte-Höller I, Wesseling P, Van Nostrand WE, Sorg C, Ruiter DJ, de Waal RMW: A lysosomal marker for activated microglial cells involved in Alzheimer classic senile plaques. Acta Neuropathol 1995, 90:493−503
11. Norton WT, Aquino DA, Hozumi I, Chiu FC, Brosnan CF: Quantitative aspects of reactive gliosis: a review. Neurochem Res 1992, 17: 877−885
12. Sofroniew MV, Vinters HV: Astrocytes: biology and pathology. Acta Neuropathol 2010, 119:7−35
13. McKhann G, Drachman D, Folstein M, Katzman R, Price D, Stadlan EM: Clinical diagnosis of Alzheimer's disease: report of the NINCDS-ADRDA Work Group under the auspices of the Department of Health and Human Services Task Force on Alzheimer's Disease. Neurology 1984, 34:939−944
14. Consensus recommendations for the postmortem diagnosis of Alzheimer's disease. The National Institute of Aging, and Reagan Institute Working Group on Diagnostic Criteria for the Neuropathological Assessment of Alzheimer's Disease. Neurobiol Aging 1997, 18(4 Suppl):S1−S2
15. Gerdes J, Lemke H, Baisch H, Wacker HH, Schwab U, Stein H: Cell cycle analysis of a cell proliferation-associated human nuclear antigen defined by the monoclonal antibody Ki-67. J immunol 1984, 133: 1710−1715
16. Cattoretti G, Becker MH, Key G, Duchrow M, Schlüter C, Galle J, Gerdes J: Monoclonal antibodies against recombinant parts of the Ki-67 antigen (MIB 1 and MIB 3) detect proliferating cells in microwave-processed formalin-fixed paraffin sections. J Pathol 1992, 168:357−363
17. Freeman SH, Kandel R, Cruz L, Rozkalne A, Newell K, Frosch MP, Hedley-Whyte ET, Locascio JJ, Lipsitz LA, Hyman BT: Preservation of neuronal number despite age-related cortical brain atrophy in elderly subjects without Alzheimer disease. J Neuropathol Exp Neurol 2008, 67:1205−1212
18. Arriagada PV, Growdon JH, Hedley-Whyte ET, Hyman BT: Neurofibrillary tangles but not senile plaques parallel duration and severity of Alzheimer's disease. Neurology 1992, 42:631−639
19. Gómez-Isla T, Hollister R, West H, Mui S, Growdon JH, Petersen RC, Parisi JE, Hyman BT: Neuronal loss correlates with but exceeds neurofibrillary tangles in Alzheimer's disease. Ann Neurol 1997, 41:17−24
20. Ingelsson M, Fukumoto H, Newell KL, Growdon JH, Hedley-Whyte ET, Frosch MP, Albert MS, Hyman BT, Irizarry MC: Early Abeta accumulation and progressive synaptic loss, gliosis, and tangle formation in AD brain. Neurology 2004, 62:925−931
21. Serrano-Pozo A, Mielke ML, Gómez-Isla T, Betensky RA, Growdon JH, Frosch MP, Hyman BT: Reactive glia not only associates with plaques but also parallels tangles in Alzheimer's disease. Am J Pathol 2011, 179:1373−1384
22. Robinson SR: Neuronal expression of glutamine synthetase in Alzheimer's disease indicates a profound impairment of metabolic interactions with astrocytes. Neurochem Int 2000, 36:471−482
23. Mattiace LA, Davis P, Dickson DW: Detection of HLA-DR on microglia in the human brain is a function of both clinical and technical factors. Am J Pathol 1990, 136:1101−1114
24. Egensperger R, Kösel S, von Eitzen U, Graeber MB: Microglial activation in Alzheimer disease: association with APOE genotype. Brain Pathol 1998, 8:439−447
25. Hyman BT, Gómez-Isla T, Irizarry MC: Stereology: a practical primer for neuropathology. J Neuropathol Exp Neurol 1998, 57: 305−310
26. Pelvig DP, Pakkenberg H, Regeur L, Oster S, Pakkenberg B: Neocortical glial cell numbers in Alzheimer's disease. Dement Geriatr Cogn Disord 2003, 16:212−219
27. Nagy Z, Esiri MM, Smith AD: Expression of cell division markers in the hippocampus in Alzheimer's disease and other neurodegenerative conditions. Acta Neuropathol 1997, 93:294−300
28. Wharton SB, Williams GH, Stoeber K, Gelsthorpe CH, Baxter L, Johnson AL, Ince PG; MRC Cognitive Function and Ageing Neuropathology Study Group: Expression of Ki67, PCNA and the chromosome replication licensing protein Mcm2 in glial cells of the aging human hippocampus increases with the burden of Alzheimer-type pathology. Neurosci Lett 2005, 383:33−38
29. Boekhoorn K, Joels M, Lucassen PJ: Increased proliferation reflects glial and vascular-associated changes, but not neurogenesis in the presenile Alzheimer hippocampus. Neurobiol Dis 2006, 24:1−14
30. Gärtner U, Brückner MK, Krug S, Schmetsdorf S, Staufenbiel M, Arendt T: Amyloid deposition in APP23 mice is associated with the expression of cyclins in astrocytes but not in neurons. Acta Neuropathol 2003, 106:535−544
31. Bondolfi L, Calhoun M, Ermini F, Kuhn G, Wiederhold KH, Walker L, Staufenbiel M, Jucker M: Amyloid-associated neuron loss and gliogenesis in the neocortex of amyloid precursor protein transgenic mice. J Neurosci 2002, 22:515−522
32. Luccarini I, Grossi C, Traini C, Fiorentini A, Dami TE, Casamenti F: Abeta plaque-associated glial reaction as a determinant of apoptotic neuronal death and cortical gliogenesis: a study in APP mutant mice. Neurosci Lett 2012, 506:94−99
33. Kamphuis W, Orre M, Kooijman L, Dahmen M, Hol EM: Differential cell proliferation in the cortex of the APPswePS1dE9 Alzheimer's disease mouse model. Glia 2012, 60:615−629
34. Simpson JE, Ince PG, Lace G, Forster G, Shaw PJ, Matthews F, Savva G, Brayne C, Wharton SB; MRC Cognitive Function and Ageing Neuropathology Study Group: Astrocyte phenotype in relation to Alzheimer-type pathology in the ageing brain. Neurobiol Aging 2010, 31:578−590
35. Kashon ML, Ross GW, O'Callaghan JP, Miller DB, Petrovich H, Burchfiel CM, Sharp DS, Markesbery WR, Davis DG, Hardman J, Nelson J, White LR: Associations of cortical astrogliosis with cognitive performance and dementia status. J Alzheimers Dis 2004, 6: 595−604
36. Wyss-Coray T: Inflammation in Alzheimer disease: driving force, bystander or beneficial response? Nat Med 2006, 12:1005−1015
37. Paolicelli RC, Bolasco G, Pagani F, Maggi L, Scianni M, Panzanelli P, Giustetto M, Ferreira TA, Guiducci E, Dumas L, Ragozzino D, Gross CT: Synaptic pruning by microglia is necessary for normal brain development. Science 2011, 333:1456−1458
38. Schafer DP, Lehrman EK, Kautzman AG, Koyama R, Mardinly AR, Yamasaki R, Ransohoff RM, Greenberg ME, Marres BA, Stevens B: Microglia sculpt postnatal neural circuits in an activity and complement-dependent manner. Neuron 2012, 74:691−705
39. Tsai HH, Li H, Fuentealba LC, Molofsky AV, Taveira-Marques R, Zhuang H, Tenney A, Mumen AT, Fancy SP, Merkle F, Kessaris N, Alvarez-Buylla A, Richardson WD, Rowitch DH: Regional astrocyte allocation regulates CNS synaptogenesis and repair. Science 2012, 337:358−362

40. Kuchibhotla KV, Lattarulo CR, Hyman BT, Bacskai BJ: Synchronous hyperactivity and intercellular calcium waves in astrocytes in Alzheimer mice. Science 2009, 323:1211−1215
41. Fuhrmann M, Bittner T, Jung CK, Burgold S, Page RM, Mitteregger G, Haass C, LaFerla FM, Kretzschmar H, Herms J: Microglial Cx3cr1 knockout prevents neuron loss in a mouse model of Alzheimer disease. Nat Neurosci 2010, 13:411−413
42. Furman JL, Sama DM, Gant JC, Beckett TL, Murphy MP, Bachstetter AD, Van Eldick LJ, Norris CM: Targeting astrocytes ameliorates neurologic changes in a mouse model of Alzheimer's disease. J Neurosci 2012, 32:16129−16140
43. Kraft AW, Hu X, Yoon H, Yan P, Xiao Q, Wang Y, Gil SC, Brown J, Wilhelmsson U, Restivo JL, Cirrito JR, Holtzman DM, Kim J, Pekny M, Lee JM: Attenuating astrocyte activation accelerates plaque pathogenesis in APP/PS1 mice. FASEB J 2013, 27:187−198
44. Graeber MB, Streit WJ, Büringer D, Sparks L, Kreutzberg GW: Ultrastructural location of major histocompatibility complex (MHC) class II positive perivascular cells in histologically normal human brain. J Neuropathol Exp Neurol 1992, 51:303−311
45. Perlmutter LS, Scott SA, Barrón E, Chui HC: MHC class II-positive microglia in human brain: association with Alzheimer lesions, [Erratum appeared in J Neurosci Res 1993, 35:346]. J Neurosci Res 1992, 33:549−558
46. Malm TM, Koistinaho M, Pärepalo M, Vatanen T, Ooka A, Karlsson S, Koistinaho J: Bone-marrow-derived cells contribute to the recruitment of microglial cells in response to beta-amyloid deposition in APP/PS1 double transgenic Alzheimer mice. Neurobiol Dis 2005, 18:134−142
47. Stalder AK, Ermini F, Bondolfi L, Krenger W, Burbach GJ, Deller T, Coomaraswamy J, Staufenbiel M, Landmann R, Jucker M: Invasion of hematopoietic cells into the brain of amyloid precursor protein transgenic mice. J Neurosci 2005, 25:11125−11132
48. Simard AR, Soulet D, Gowing G, Julien JP, Rivest S: Bone marrow-derived microglia plays a critical role in restricting senile plaque formation in Alzheimer's disease. Neuron 2006, 49:489−502
49. Mildner A, Schlevogt B, Kierdorf K, Böttcher C, Erny D, Kummer MP, Quinn M, Brück W, Bechmann I, Heneka MT, Priller J, Prinz M: Distinct and non-redundant roles of microglia and myeloid subsets in mouse models of Alzheimer's disease. J Neurosci 2011, 31: 11159−11171
50. Wisniewski HM, Kozlowski PB: Evidence for blood-brain barrier changes in senile dementia of the Alzheimer type (SDAT). Ann N Y Acad Sci 1982, 396:119−129
51. Alafuzoff I, Adolfsson R, Grundke-Iqbal I, Winblad B: Blood-brain barrier in Alzheimer dementia and in non-demented elderly. Acta Neuropathol 1987, 73:160−166
52. Viggars AP, Wharton SB, Simpson JE, Matthews FE, Brayne C, Savva GM, Garwood C, Drew D, Shaw PJ, Ince PG: Alterations in the blood brain barrier in ageing cerebral cortex in relationship to Alzheimer-type pathology: a study in the MRC-CFAS population neuropathology cohort. Neurosci Lett 2011, 505:25−30
53. Skoog I, Wallin A, Fredman P, Hesse C, Aevarsson O, Karlsson I, Gottfries CG, Blennow K: A population study on blood-brain barrier function in 85-year-olds: relation to Alzheimer's disease and vascular dementia. Neurology 1998, 50:966−971
54. Algotsson A, Winblad B: The integrity of the blood-brain barrier in Alzheimer's disease. Acta Neurol Scand 2007, 115:403−408
55. Bowman GL, Kaye JA, Moore M, Waichunas D, Carlson NE, Quinn JF: Blood-brain barrier impairment in Alzheimer disease: stability and functional significance. Neurology 2007, 68:1809−1814
56. Cudaback E, Li X, Montine KS, Montine TJ, Keene CD: Apolipoprotein E isoform-dependent microglia migration. FASEB J 2011, 25: 2082−2091
57. Vitek MP, Brown CM, Colton CA: APOE genotype-specific differences in the innate immune response. Neurobiol Aging 2009, 30: 1350−1360
58. Zhu Y, Nwabuisi-Heath E, Dumanis SB, Tai LM, Yu C, Rebeck GW, LaDu MJ: APOE genotype alters glial activation and loss of synaptic markers in mice. Glia 2012, 60:559−569
59. Maeda J, Zhang MR, Okauchi T, Ji B, Ono M, Hattori S, Kumata K, Iwata N, Saido TC, Trojanowski JQ, Lee VM, Staufenbiel M, Tomiyama T, Mori H, Fukumura T, Suhara T, Higuchi M: In vivo positron emission tomography imaging of glial responses to amyloid-beta and tau pathologies in mouse models of Alzheimer's disease and related disorders. J Neurosci 2011, 31:4720−4730
60. Lavisse S, Guillermier M, Hérard AS, Petit F, Delahaye M, Van Camp N, Ben Haim L, Lebon V, Remy P, Dollé F, Delzescaux T, Bonvento G, Hantraye P, Escartin C: Reactive astrocytes overexpress TSPO and are detected by TSPO positron emission tomography imaging. J Neurosci 2012, 32:10809−10818
61. Venneti S, Lopresti BJ, Wiley CA: Molecular imaging of microglia/macrophages in the brain. Glia 2012, 61:10−23
62. Wiley CA, Lopresti BJ, Venetti S, Price J, Klunk WE, DeKosky ST, Mathis CA: Carbon 11-labeled Pittsburgh compound B and carbon 11-labeled (R)-PK11195 positron emission tomographic imaging in Alzheimer disease. Arch Neurol 2009, 66:60−67
63. Schuitemaker A, Kropholler MA, Boellaard R, van der Flier WM, Kloet RW, van der Doef TF, Knol DL, Windhorst AD, Luurtsema G, Barkhof F, Jonker C, Lammertsma AA, Scheltens P, van Berckel BN: Microglial activation in Alzheimer's disease: an (R)-[^{11}C]PK11195 positron emission tomography study. Neurobiol Aging 2013, 34: 128−136